

Temperature echoes revisited to probe the vibrational behavior of dendrimers

Cite as: J. Chem. Phys. **132**, 114901 (2010); <https://doi.org/10.1063/1.3353952>

Submitted: 29 September 2009 • Accepted: 13 February 2010 • Published Online: 16 March 2010

Pedro M. R. Paulo



View Online



Export Citation

ARTICLES YOU MAY BE INTERESTED IN

[Are structural properties of dendrimers sensitive to the symmetry of branching? Computer simulation of lysine dendrimers](#)

The Journal of Chemical Physics **139**, 064903 (2013); <https://doi.org/10.1063/1.4817337>

[Structured water in polyelectrolyte dendrimers: Understanding small angle neutron scattering results through atomistic simulation](#)

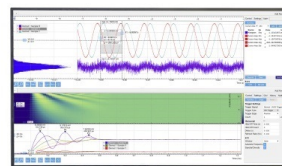
The Journal of Chemical Physics **136**, 144901 (2012); <https://doi.org/10.1063/1.3697479>

[Effect of counterion valence on the pH responsiveness of polyamidoamine dendrimer structure](#)

The Journal of Chemical Physics **132**, 124901 (2010); <https://doi.org/10.1063/1.3358349>

Challenge us.

What are your needs for
periodic signal detection?



Zurich
Instruments



Temperature echoes revisited to probe the vibrational behavior of dendrimers

Pedro M. R. Paulo^{a)}

Centro de Química Estrutural - Complexo I, Instituto Superior Técnico, Av. Rovisco Pais, 1049-001 Lisboa, Portugal

(Received 29 September 2009; accepted 13 February 2010; published online 16 March 2010)

Temperature quench echoes were induced in molecular dynamics simulations of dendrimers. This phenomenon was used to probe the vibrational behavior of these molecules by comparing simulation results with harmonic model predictions. The echo depth for short time intervals between temperature quenches is well described by the harmonic approximation and the fluctuations observed are related to the vibrational density of states. The echo depth for long time intervals decays progressively revealing dephasing due to anharmonic interactions. The density of states was calculated from the temperature fluctuations after the first quench and high-frequency modes were assigned by comparison with vibrational spectra of similar dendrimers. © 2010 American Institute of Physics. [doi:10.1063/1.3353952]

I. INTRODUCTION

Computational models provide a valuable tool for the study of motion in complex or disordered systems, such as amorphous solids, polymer glasses, or proteins. Normal mode analysis is an example of a method generally used for this purpose.^{1–7} Although this method gives detailed insight on vibrational motion, it neglects anharmonic contributions and is of limited use to describe dynamics of systems with complex potential energy surfaces. In this case, the methods based on molecular dynamics simulations,^{8–16} such as the temperature echoes,^{17–23} are better suited.

The standard procedure to induce a temperature echo in a simulation consists of a double temperature quench. Starting from a system equilibrated at temperature T_0 , the kinetic energy is instantaneously removed at instant $t=0$ by setting the velocity of all particles to zero. Immediately after the quench, the temperature is zero but then the system evolves to equilibrium, as potential energy is converted to kinetic energy. The new equilibrium temperature is approximately $T_0/2$, in agreement with the equipartition principle. After some time interval $t=\tau$, the kinetic energy of the system is again removed causing a second temperature quench. The echo is then observed at instant $t=2\tau$ as a short decrease in the temperature trajectory (Fig. 1).

The first quench creates a coherent vibrational state or, using a normal mode picture, it resets each mode to a phase 0 or π . The modes with a frequency corresponding to a multiple of π/τ have zero kinetic energy at the instant of the second quench and, therefore, are not affected by this quench. At instant 2τ , these modes have again zero kinetic energy and this contributes to the appearance of the temperature echo. The second quench acts as a filter of the energy spectrum by selecting modes with frequencies nearby $n\pi/\tau$.²⁴ In this sense, it was originally proposed that tem-

perature quench echoes could be used to obtain individual normal modes and assess the density of states.

Temperature echoes were first detected in simulations of Lennard-Jones glasses.^{17,18} By applying multiple quench steps, it was possible to isolate normal modes in these systems. The degree of localization of the modes was characterized as a function of mode frequency. There is a transition between localized and extended modes, which occurs over a narrow interval, as frequency decreases. Temperature echoes were later observed in simulations of proteins.^{22,23} These systems are more inhomogeneous than simple glasses due to chemical bond and long range electrostatic interactions. Low frequency modes are particularly interesting because they are related to collective motion of several atoms across the protein. This type of extended motion could be involved in triggering conformational changes, such as protein unfolding. In this contribution, we revisit the temperature echo phenomenon in a different kind of macromolecular system.

Dendrimers are artificial polymers with a highly ramified structure.^{25,26} These molecules are built around a core unit by adding successive layers of repeating units, usually called generations, according to a self-similar motif (Fig. 2). Dendrimers with flexible repeating units have a globular shape and their size is around a few nanometers. Such features are comparable to small proteins, but the lack of secondary or tertiary structure renders dendrimers much less organized than proteins. Some dendrimers display an interesting antenna effect, where efficient migration of phonon energy, supplied by infrared radiation, occurs from the dendrimer's periphery to its core.^{27,28} This behavior is not obvious because the branching structure of the dendrimer imposes an entropic penalty for energy migration toward the core. A plausible explanation for this antenna effect invokes anisotropic vibronic coupling between repeating units due to close molecular packing at the dendrimer's periphery (cf. Fig. 2). Although phonon-antenna effects are not known for the type of dendrimers modeled in our simulations, we considered

^{a)}Electronic mail: pedro.m.paulo@ist.utl.pt.

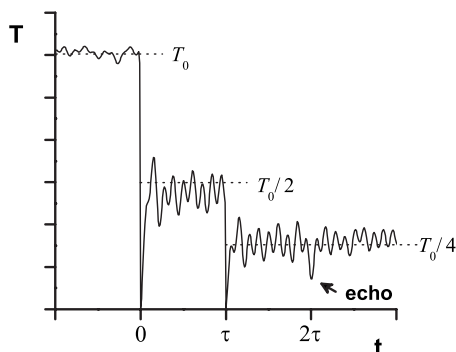


FIG. 1. Temperature trajectory from molecular dynamics simulations of a dendrimer showing the double quench at times 0 and τ followed by the temperature echo at instant 2τ .

dendrimers with different number of repeating units (or generations) to investigate possible effects from molecular packing in the vibrational behavior of these systems. Indeed, we have noticed in our temperature echo simulations that the vibrational density of states of the simulated dendrimers shows frequency shifts and peak broadening with increasing dendrimer generation. Some of these results maybe experimentally confirmed, by measuring infrared spectra or inelastic neutron scattering spectra, of a series of dendrimer generations. More generally, this paper illustrates the potential of temperature echo simulation technique in the study of soft matter. Previous studies with protein model systems had already suggested the potential of this technique for studying motion in macromolecular systems.^{22,23} In this sense, dendrimers are interesting model systems because they are chemically simpler and less organized than proteins, but have a well defined branching structure that can be grown in a self-similar scheme. This allows to probe size effects in disordered soft systems with a high degree of chemical bonding and supramolecular interactions, as dendrimers are. Other systems, such as hyperbranched or star polymers, could also be interesting probe systems for temperature echo studies.

Our interest in dendrimers was motivated by previous spectroscopic studies of photoinduced electron-transfer in porphyrin-dendrimer supramolecular systems.²⁹ The role of conformational changes and dielectric relaxation associated with electron transfer in these systems was investigated before using molecular dynamics simulations.³⁰ In this contri-

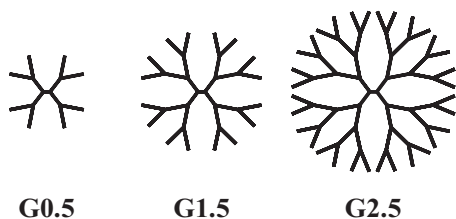


FIG. 2. Scheme illustrating the self-similar structure of dendrimer generations G0.5, G1.5, and G2.5 (each segment represents $-\text{CH}_2-\text{CH}_2-\text{CO}-\text{NH}-\text{CH}_2-\text{CH}_2-\text{NH}-$ except for the core $>\text{N}-\text{CH}_2-\text{CH}_2-\text{N}<$ and the terminal segments $-\text{CH}_2-\text{CH}_2-\text{COO}^-$). Notice the more compact packing near the periphery as the dendrimer generation increases, perceptible even in this simple schematic form.

bution, we further explore the behavior of dendrimer systems by using the temperature echo simulation technique.

II. MODEL AND METHODS

The dendrimer model used in our simulations is described in Ref. 31. Briefly, it is an atomistic model of poly(amido)amine or PAMAM dendrimers based on OPLS and AMBER force fields. Five dendrimer sizes or generations were considered with a total number of 148, 356, 772, 1604, and 3268 atoms. These generations are abbreviated as $Gn.5$ with $n=0, \dots, 4$, respectively. Initial configurations for each generation were selected from equilibrated structures of previous simulations with duration of several hundred picoseconds.³¹ Distance constraints imposed before on bonds involving H atoms were lifted and the simulation time step was decreased to 0.5 fs. During the initial stage of equilibration, which lasted several tens of picoseconds in a NVT ensemble, the temperature was maintained around 300 K by coupling the system to a Nosé–Hoover thermostat. Then, the thermostat was disconnected and the simulation was extended for a similar period as a microcanonical, NVE , ensemble. From the last 5 ps of simulation, six configurations were sampled at equal time intervals and were used for the temperature echo simulation runs. The double-quench procedure described before was used for inducing the echoes and the results presented here are the average from the six sampled configurations. The simulations were performed with DL_POLY program. No explicit solvent was introduced, but the dielectric constant of water was used for calculating electrostatic interactions. These were handled with the Ewald method using a cutoff distance of 50 Å. The radius of gyration calculated for the dendrimers in our simulations³¹ is comparable to values obtained in other simulations with implicit solvent.³² The introduction of explicit solvent leads to swelling of the dendrimer and to better agreement with experimental values of dendrimer radius.^{33–35} However, the use of implicit solvent allows to define simulation cells with larger sizes (which are more comparable to experimental conditions) and, thus, to reproduce more realistically the spatial distribution of counterions around the dendrimer.^{31,35}

Temperature echoes can be predicted from a classical harmonic model, as it was originally shown by Rahman and co-workers^{17–20} and later reformulated by Xu *et al.*²³ Here we briefly outline some of their results. For a system with N particles or atoms, each of the $3N-6$ internal normal modes is described by a harmonic oscillator with a frequency ω_i for the i th mode. The evolution of temperature after the first quench ($0 \leq t < \tau$) is

$$T_1(t) = \frac{T_0}{2} [1 - \langle \cos(2\omega_i t) \rangle_I], \quad (1)$$

where T_0 is the equilibrium temperature of the system before the quench and the angle brackets indicate the average over all normal modes, $\langle f(\omega_i) \rangle_I = (3N-6)^{-1} \sum_i f(\omega_i)$.

After the second quench ($t \geq \tau$), the temperature is given by

$$T_2(t) = \frac{T_0}{4} \left\{ 1 - \langle \cos[2\omega_i(t - \tau)] \rangle_I + \langle \cos(2\omega_i\tau) \rangle_I - \frac{1}{2} \langle \cos(2\omega_i t) \rangle_I - \frac{1}{2} \langle \cos[2\omega_i(t - 2\tau)] \rangle_I \right\}. \quad (2)$$

The last term of this expression reaches the most negative value at $t=2\tau$ and it explains the temperature echo. Xu *et al.*²³ have shown that, within the harmonic approximation, the cosine terms in expression (2) are related to the temperature autocorrelation function $C(t)$ through

$$\langle \cos(2\omega_i t) \rangle_I = C(t) \equiv \frac{\langle T_0(t)T_0(0) \rangle - \langle T_0(t) \rangle^2}{\langle [T_0(t)]^2 \rangle - \langle T_0(t) \rangle^2}, \quad (3)$$

where $T_0(t)$ is the temperature trajectory of the equilibrated system before any quenches. The function $C(t)$ can be directly evaluated from molecular dynamics simulations and the same is valid for $T_2(t)$ by replacing the definition of $C(t)$ in expression (2) to obtain

$$T_2(t) = \frac{T_0}{4} \left[1 - C(t - \tau) + C(\tau) - \frac{1}{2}C(t) - \frac{1}{2}C(|t - 2\tau|) \right]. \quad (4)$$

Furthermore, by rewriting the average over all normal modes of the cosine terms as a continuous approximation for a large number of modes,

$$C(t) = \langle \cos(2\omega_i t) \rangle_I \approx \int_0^\infty D(\omega) \cos(2\omega t) d\omega, \quad (5)$$

it becomes clear that the density of states $D(\omega)$ of a harmonic system can be evaluated from the inverse cosine Fourier transform of the temperature autocorrelation function. Another means to accomplish the same was suggested by Grest *et al.*¹⁹ using the following function:

$$K(t) = \left\langle 1 - \frac{T_1(t)}{T_{1\infty}} \right\rangle_Z \approx \int_0^\infty D(\omega) \cos(2\omega t) d\omega, \quad (6)$$

where $\langle \dots \rangle_Z$ indicates an ensemble average, $T_1(t)$ is the temperature trajectory after the first quench, and $T_{1\infty}$ is the equilibrium temperature after a single quench, which is approximately $T_0/2$ as previously mentioned. Comparing expressions (5) and (6), the following identity $K(t)=C(t)$ can be established for a purely harmonic system. The simulated systems are not purely harmonic due to torsional, electrostatic, and van der Waals interactions that contribute to coupling between normal modes. However, the harmonic approximation can still give valuable insights regarding vibrational motion in the simulated systems.

III. RESULTS AND DISCUSSION

Temperature echoes were monitored in dendrimer simulations for time delays between quenches as short as 0.02 up to 1.5 ps.³⁶ An example of a temperature trajectory showing an echo for a short time delay is given in Fig. 1. After each quench, the temperature rises rapidly and within a few femtoseconds it almost reaches the new equilibrium value. However, there are strong temperature fluctuations that persist for

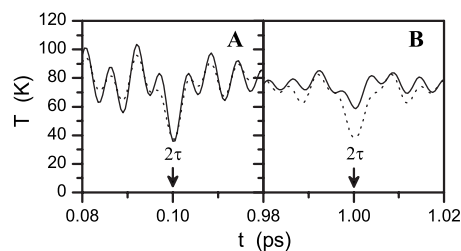


FIG. 3. Detailed view of the temperature echoes observed for dendrimer generation G2.5 for time delays between quenches of (a) $\tau=0.05$ ps and (b) $\tau=0.5$ ps. The full line represents the simulated temperature trajectory averaged over six runs and the dashed line depicts the predictions from the harmonic model calculated with Eq. (4).

much longer. These fluctuations carry information about the density of states of the system.³⁷ A detailed view of the echo in Fig. 1 is shown in Fig. 3(a). For short time delays, the harmonic model gives a reasonably good description of the echo profile [dashed line, Fig. 3(a)]. In the short time range, the behavior of the system is dominated by the high frequency modes that are usually “good” normal modes, which explains the success of the harmonic approximation.

The width of the echo is determined by the highest frequency mode of the system.³⁸ For the simulated dendrimers, it corresponds to the N—H stretching mode of the amide groups with a frequency around 3330 cm^{-1} , which agrees with the observed echo width of approximately 5 fs.

The depth of the echo varies significantly with the time delay between quenches. This quantity is defined as, $\Delta T_{\text{echo}} = T_{2\infty} - T_2(2\tau)$, where $T_{2\infty}$ is the equilibrium temperature after the second quench and $T_2(2\tau)$ is the temperature at the time of the echo. The values “measured” for one of the simulated dendrimers in the range of short time delays are represented in Fig. 4 (open symbols). The fluctuations observed here are related to the density of states of the system. This relation can be derived from the harmonic approximation by noticing that $T_{2\infty} = T_0/4$ and rewriting $T_2(2\tau)$ from expressions (2) and (5) to obtain

$$\Delta T_{\text{harm}} = \frac{T_0}{8} \left[1 + \int_0^\infty D(\omega) \cos(4\omega\tau) d\omega \right]. \quad (7)$$

The echo depth for a harmonic system can be estimated from expression (7) by replacing the integral with either $C(2\tau)$ or $K(2\tau)$ function (see Fig. S1 in supplementary material³⁹). A good agreement is found between the measured echo depths and predictions from the harmonic model for time delays up

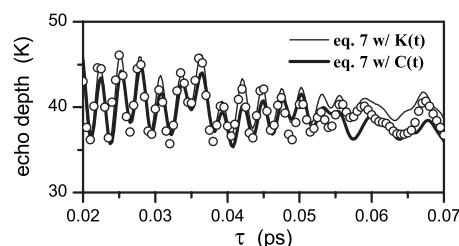


FIG. 4. Echo depth observed in simulations of dendrimer generation G2.5 (open symbols) and comparison with predictions from the harmonic model calculated with Eq. (7) using function $C(t)$ (full line) or function $K(t)$ (thin line).

to about 50 fs (solid and thin curves, Fig. 4). For longer time delays, the measured values begin to deviate significantly from the harmonic model due to buildup of anharmonic contributions.

The effect of anharmonicity in the temperature echoes is exemplified in Fig. 3(b). As the time delay between quenches is increased, there is a progressive decay of the echo depth relatively to harmonic model predictions [dashed line, Fig. 3(b)]. In this time range, the double-quench procedure probes low frequency modes, which typically involve the collective motion of several particles across the system. Anharmonic coupling between these modes is promoted by torsional, electrostatic, and van der Waals interactions in the simulated systems. This phenomenon destroys the vibrational coherence created by the double-quench procedure and, as a consequence, the temperature echo fades.

The echo depth in the dendrimer systems decays exponentially for long time delays between quenches (see Fig. S2 in supplementary material³⁹). This feature was also observed for Lennard-Jones glasses and proteins.^{17–20,22,23} Xu *et al.*²³ proposed an explanation based on a model which assumes that anharmonic interactions introduce a random phase in the motion of each oscillator and that the time evolution of this random phase is described by a diffusion equation. According to this model, the echo depth decays as $\Delta T_{\text{anharm}} = T_0/8 \exp(-\tau/\tau_c)$, where the characteristic decay time is given by $\tau_c = (3\gamma_0 k_B T_0)^{-1}$ and γ_0 is a mobility constant related to dispersion of the random phases.⁴⁰

The decay times τ_c obtained for the dendrimer systems vary between 0.52 and 0.69 ps. These values are comparable to the value of 0.83 ps obtained for the protein bovine pancreatic trypsin inhibitor (BPTI).²³ Some speculative remarks can be put forward to explain the slightly lower τ_c of the dendrimers in comparison to BPTI protein. The dendrimers are less organized than proteins and this could favor anharmonic coupling through torsional interactions. The total charge of these macromolecules can also differ significantly. Each terminal group of the dendrimer can be potentially charged, which means structural charges of 8, 16, 32, 64, and 128e for generations G0.5 to G4.5. However, the effective charge is lower due to counterion condensation that renormalizes the dendrimer charge to estimated values of 8, 13, 16, 20, and 23e for the same generations.³¹ The charge of BPTI in the simulation model is not known, but the experimental value of 6e is relatively lower than that of dendrimers.⁴¹ This difference in effective charges may suggest that there are different contributions of electrostatic interactions to anharmonic coupling in the dendrimers, as compared to those in BPTI protein.

The values of τ_c for the dendrimers seem to correlate inversely with the volume density of oscillators (Fig. 5). Intuitively, the anharmonic contributions from electrostatic and van der Waals interactions should be proportional to the number of interacting particles and, inversely, to the distance between them. The volume density of oscillators seems to account for this simple reasoning.⁴²

The conformation of dendrimers changes with increasing generation. Lower generations have more open structures and an ellipsoidal prolate shape. Higher generations are more

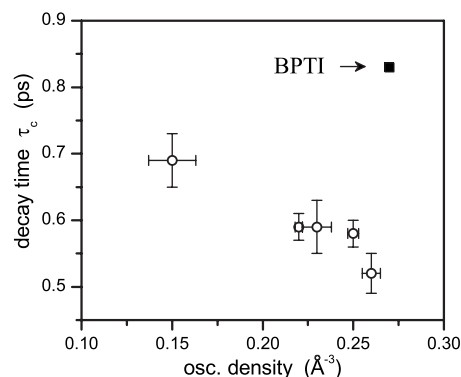


FIG. 5. Characteristic decay times of the echo depth at long time delays between quenches as a function of the volume density of oscillators for the several dendrimer generations simulated (open circles). The error bars represent the estimated standard deviation. The value of τ_c for BPTI given in Ref. 23 is also shown for comparison (closed square).

compact and spherical due to stereochemical restraints imposed by molecular packing of an exponentially increasing number of repeating units with each generation.³¹ This conformational change is likely to affect anharmonicity in dendrimers and, indeed, the value of τ_c obtained for generation 0.5 dendrimer (0.69 ps) is clearly higher than for the remaining generations (0.52–0.59 ps). Other factors that affect dendrimer conformation are the pH and salt concentration.^{34,43} It would be interesting to study how these influence anharmonicity in the simulated dendrimers through their effect on decay time τ_c .

The vibrational density of states for the simulated dendrimers was calculated from $C(t)$ or $K(t)$ using expressions (5) and (6), respectively. The spectral features obtained from either function are comparable between them, although slight differences in peak position or intensity can occur. The density of states for some of the simulated generations is shown in Fig. 6. Experimentally, this quantity can be evaluated from inelastic neutron scattering. This technique has been employed to characterize the vibrational behavior of proteins,^{44–47} but, to the best of our knowledge, it has not yet been used for dendrimers. On the other hand, there are several studies that report on infrared spectroscopy of poly(amido)amine dendrimers similar to those simulated here, and at least one on Raman spectroscopy.^{48–56} It is also known one computational study that reports on calculated infrared spectra of poly(amido)amine dendrimers, but it employs *ab initio* methods and is limited to dendrimers of the lowest generation 0.⁵⁷ These studies provide a basis for comparison with our simulation results, although infrared and Raman spectra reflect specific selection rules and, thus, are not directly comparable to the calculated density of states. Furthermore, we notice that simulations with implicit solvent do not account for specific solvent effects, such as hydrogen bonding. Molecular dynamics simulations with explicit water solvent molecules could give some insight about these effects and might complement the results presented here.

The highest frequency mode in Fig. 6 appears at 3330 cm⁻¹ and, as previously referred, corresponds to N—H stretching of the amide groups. The next peak occurs around 3000 cm⁻¹ and its assignment is not clear [peak (a)]

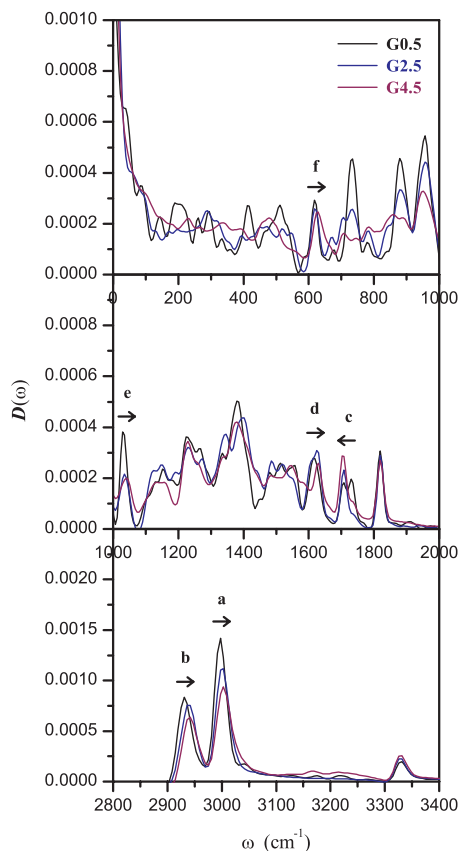


FIG. 6. Vibrational density of states for selected dendrimer generations G0.5, G2.5, and G4.5 calculated from the temperature fluctuations after the first quench using Eq. (6) with function $K(t)$. The arrows indicate the frequency shift observed with increasing dendrimer generation for some of the identified modes: (a) N—H stretching, (b) C—H stretching, [(c) and (d)] amide I, (e) CH₂ rocking, and (f) amide V and VI.

in Fig. 6]. In the infrared spectra of poly(amido)amine dendrimers, there is a band at 3080 cm⁻¹ that has been attributed to an overtone of the amide II mode⁵⁵ (i.e., a combination of N—H in-plane bending and C—N stretching) or, alternatively, to N—H stretching.⁵⁰ Close to the peak at 3000 cm⁻¹, there is another one around 2940 cm⁻¹ that has contributions from symmetric and asymmetric C—H stretching of methylene groups [peak (b)]. This peak shifts slightly to higher frequencies (about 10 cm⁻¹) with increasing dendrimer size or generation. There are at least two other peaks that show similar behavior: one at 1620 and another at 620 cm⁻¹ [peaks (d) and (f), respectively]. The former is attributed to amide I mode (i.e., C=O stretch with some in-plane C—N—H angle bending) and the latter to a combination of amide V and VI modes (i.e., respectively, N—H and C=O wagging). Another example, although not so clear, is the peak at 1030 cm⁻¹ [peak (e)] that is assigned to CH₂ rocking or, alternatively, to C—C stretching. This peak shifts only 6 cm⁻¹ to higher frequency from generation G0.5 to G4.5, but this shift is accompanied by broadening. Yet another example is the double peak structure around 1720 cm⁻¹ [peak (c)] that is attributed to amide I mode. With increasing generation, the peak at higher frequencies diminishes and becomes only a shoulder. The peak changes just described are qualitatively identical for both density of states calculated from $C(t)$ and $K(t)$. These changes occur

with increasing dendrimer size (or generation) and most likely reflect the dendrimer conformational change from a sparse to compact structure. Conformational effects have been observed in *ab initio* calculations of generation 0 dendrimers that showed frequencies shifts up to 20–30 cm⁻¹ between different dendrimer conformations. Within the same generation, the dendrimer conformational manifold should lead to inhomogeneous broadening due to different environments provided by the dendrimer itself to each vibrational mode. In particular, vibrational coupling through intramolecular hydrogen bonding should depend significantly on the orientation of dendrimer branches.⁵⁷ With increasing dendrimer generation, other effects could come into play. The molecular crowding that occurs for higher generations can impose a tension on the branches close to the dendrimer core that stretch out to increase the molecular volume and accommodate the large number of repeating units at the dendrimer's periphery. The increase of molecular strain with dendrimer size suggests a plausible explanation for the changes observed in the density of states with increasing generation, but it lacks a more detailed verification by complementary experimental and theoretical approaches.

In general, the features identified in the calculated density of states find a correspondence in experimental or calculated infrared spectra of these dendrimers. However, there are two exceptions. One is the peak situated at 1820 cm⁻¹ for which no correspondence was found in the infrared spectra reported in the literature and that we tentatively assign to a C=O stretching mode. The other is a band that appears around 2820–2850 cm⁻¹ in infrared spectra from symmetric C—H stretching of CH₂ groups, which cannot be accurately determined in the calculated density of states.

The interpretation is more difficult in the fingerprint region (below 1000 cm⁻¹) due to spectral overlap and coupling between modes. The region below 200 cm⁻¹ is particularly interesting because it contains modes that, due to their collective character, could be involved in conformational rearrangement of dendrimer branches. There remains the doubt about enough sampling of the dendrimer conformational space to obtain a reliable characterization of these modes in simulations of several picoseconds. The many conformational degrees of freedom associated with the fractal chemical structure of the dendrimer suggests a rough potential energy surface with many quasi-isoenergetic minima. Low frequency modes could be involved in crossing energy barriers between minima. Some of these modes could have imaginary frequency corresponding to saddle points in the potential energy surface. Friction acting on these modes from interaction with other dendrimer branches can lead to an overdamped motion, which is more of a restrained diffusion character than vibrational. Characterization of the motion involved in these modes could be important, for instance, to understand dielectric relaxation accompanying electron transfer in dendrimer systems, in which case slow relaxation components of a few picoseconds (<20 ps) have been observed in molecular dynamics simulations.³⁰

IV. CONCLUSIONS

Temperature quench echoes were originally demonstrated in simulations of Lennard-Jones glasses almost three decades ago. Since then, modified versions of this method and other related methods have been developed. An example is the velocity reassignment echo procedure, which uses correlated sets of velocities to probe vibrational motion in simulated systems with only a mild perturbation in their temperature.⁵⁸ Another example relies on multiple kinetic and potential energy quenches to isolate normal modes at low temperature and then studies energy transfer among these modes at higher temperatures.⁵⁹ In common, these methods have the possibility to address an individual subset of particles or vibrations in the simulated system and to follow dynamics of energy transfer in a more detailed manner. This could be an interesting possibility to investigate directional phonon energy migration due to anisotropic vibronic coupling in dendrimer systems.

In this contribution, we revisited the temperature echo phenomenon in simulations of dendrimers using the double quench procedure to probe the vibrational behavior of these molecules. This approach is better suited for dendrimers and other complex molecules than, for instance, conventional *ab initio* methods combined with normal-mode analysis, due to the many conformational degrees of freedom of these systems. The characteristics of the echo at short time delays between quenches are reasonably described by the harmonic model, but with increasing time delays anharmonic contributions to motion cause the echo to fade. The echo depth decays exponentially, but with slightly different decay times for the several generations simulated. The vibrational density of states was calculated from the temperature fluctuations after the first quench assuming the harmonic approximation. The peak structure of the density of states finds correspondence to features reported in experimental and calculated infrared spectra. Some peaks shift slightly or broaden with increasing dendrimer size or generation. The increase in molecular strain due to the large number of repeating units packed in higher generations seems to be a plausible explanation for the changes observed in the density of states, but it requires further evaluation by other methods, like infrared spectroscopy or inelastic neutron scattering.

ACKNOWLEDGMENTS

This work was supported by Centro de Química Estrutural, I.S.T. under the Project No. PPCDT/QUI/57387/2004. P.M.R.P. acknowledges the post-doc Grant No. SFRH/BPD/25141/2005 from Fundação para a Ciência e a Tecnologia. The author thanks Professors S. M. B. Costa, J. N. Canongia Lopes, and L. M. Ilharco for valuable discussions.

¹B. Brooks and M. Karplus, *Proc. Natl. Acad. Sci. U.S.A.* **80**, 6571 (1983).

²M. Levitt, C. Sander, and P. S. Stern, *J. Mol. Biol.* **181**, 423 (1985).

³D. A. Case, *Curr. Opin. Struct. Biol.* **4**, 285 (1994).

⁴S. Hayward, A. Kitao, and N. Gô, *Protein Sci.* **3**, 936 (1994).

⁵B. M. Forrest, E. Leontidis, and U. W. Suter, *J. Chem. Phys.* **104**, 2401 (1996).

⁶J. C. Smith, A. Lamy, M. Kataoka, J. Yunoki, A.-J. Petrescu, V. Receveur, P. Calmettes, and D. Durand, *Physica B* **241–243**, 1110 (1998).

⁷J. Ma, *Structure (London)* **13**, 373 (2005).

⁸R. M. Levy, D. Perahia, and M. Karplus, *Proc. Natl. Acad. Sci. U.S.A.* **79**, 1346 (1982).

⁹P. Dauber-Osguthorpe and D. J. Osguthorpe, *J. Am. Chem. Soc.* **112**, 7921 (1990).

¹⁰R. B. Sessions, D. J. Osguthorpe, and P. Dauber-Osguthorpe, *J. Phys. Chem.* **99**, 9034 (1995).

¹¹D. Xu, C. Martin, and K. Schulten, *Biophys. J.* **70**, 453 (1996).

¹²S. Héry, D. Genest, and J. C. Smith, *Physica B* **234–236**, 175 (1997).

¹³S. C. Phillips, J. W. Essex, and C. M. Edge, *J. Chem. Phys.* **112**, 2586 (2000).

¹⁴D. E. Sagnella, J. E. Straub, and D. Thirumalai, *J. Chem. Phys.* **113**, 7702 (2000).

¹⁵N. Ota and D. A. Agard, *J. Mol. Biol.* **351**, 345 (2005).

¹⁶K. Sharp and J. J. Skinner, *Proteins* **65**, 347 (2006).

¹⁷G. S. Grest, S. R. Nagel, and A. Rahman, *Solid State Commun.* **36**, 875 (1980).

¹⁸S. R. Nagel, A. Rahman, and G. S. Grest, *Phys. Rev. Lett.* **47**, 1665 (1981).

¹⁹G. S. Grest, S. R. Nagel, A. Rahman, and T. A. Witten, Jr., *J. Chem. Phys.* **74**, 3532 (1981).

²⁰S. R. Nagel, G. S. Grest, and A. Rahman, *Phys. Today* **24** (1983).

²¹J. D. Bauer and D. F. Calef, *Chem. Phys. Lett.* **187**, 391 (1991).

²²O. M. Becker and M. Karplus, *Phys. Rev. Lett.* **70**, 3514 (1993).

²³D. Xu, K. Schulten, O. M. Becker, and M. Karplus, *J. Chem. Phys.* **103**, 3112 (1995).

²⁴Indeed, for systems with a broad distribution of frequencies, the contribution of modes with frequencies nearby $n\pi/\tau$ is significant, so that a double quench does not completely isolate certain modes.

²⁵D. A. Tomalia, H. Baker, J. Dewald, M. Hall, G. Kallos, S. Martin, J. Roeck, J. Ryder, and P. Smith, *Polym. J. (Tokyo, Jpn.)* **17**, 117 (1985).

²⁶A. W. Bosman, H. M. Janssen, and E. W. Meijer, *Chem. Rev. (Washington, D.C.)* **99**, 1665 (1999).

²⁷A. Okada and H. Sumi, *Chem. Phys. Lett.* **340**, 336 (2001).

²⁸K. Nishioka and M. Suzuki, *J. Chem. Phys.* **117**, 7793 (2002).

²⁹P. M. R. Paulo and S. M. B. Costa, *J. Phys. Chem. B* **109**, 13928 (2005).

³⁰P. M. R. Paulo, J. N. Canongia Lopes, and S. M. B. Costa, *J. Phys. Chem. B* **112**, 14779 (2008).

³¹P. M. R. Paulo, J. N. C. Lopes, and S. M. B. Costa, *J. Phys. Chem. B* **111**, 10651 (2007).

³²P. K. Maiti, T. Çağın, G. Wang, and W. A. Goddard III, *Macromolecules* **37**, 6236 (2004).

³³P. K. Maiti, T. Çağın, S.-T. Lin, and W. A. Goddard III, *Macromolecules* **38**, 979 (2005).

³⁴Y. Liu, V. S. Bryantsev, M. S. Diallo, and W. A. Goddard III, *J. Am. Chem. Soc.* **131**, 2798 (2009).

³⁵P. K. Maiti and R. Messina, *Macromolecules* **41**, 5002 (2008).

³⁶For time delays much below 0.02 ps, the echoes are ill defined due to relaxation of the system after each quench.

³⁷The relation between the temperature fluctuations after the first quench and the density of states is given by expression (1) combined with expressions (3) and (5).

³⁸This can be seen from expression (4) by noticing that at the time of the quench the last term $C(|t-2\tau|)$ prevails because $C(t)$ decays rapidly at short times. The echo width is thus determined by the behavior of $C(t)$ at short times, which is determined by the high frequency modes.

³⁹See supplementary material at <http://dx.doi.org/10.1063/1.3353952> for representations of functions $C(t)$ and $K(t)$ (Fig. S1) and of echo-depth decay at long time delays between quenches (Fig. S2), as described in the text.

⁴⁰This model is only approximate because there are fluctuations of the echo depth superimposed to the exponential decay, which arise from specific features of the density of states that are neglected in the model.

⁴¹J. Gao and G. M. Whitesides, *Anal. Chem.* **69**, 575 (1997).

⁴²The number of oscillators is given by $3N-6$, where N is the number of atoms in each dendrimer generation. The volume of the dendrimer was approximated to that of an ellipsoid with constant density, where the length of the axes was calculated from the principal moments of inertia of dendrimer configurations sampled from the simulations.

⁴³W. Tian and Y. Ma, *J. Phys. Chem. B* **113**, 13161 (2009).

⁴⁴S. Cusack, J. Smith, J. Finney, B. Tidor, and M. Karplus, *J. Mol. Biol.* **202**, 903 (1988).

⁴⁵J. Smith, S. Cusack, B. Tidor, and M. Karplus, *J. Chem. Phys.* **93**, 2974 (1990).

- ⁴⁶ A. V. Goupil-Lamy, J. C. Smith, J. Yunoki, S. F. Parker, and M. Kataoka, *J. Am. Chem. Soc.* **119**, 9268 (1997).
- ⁴⁷ E. Balog, T. Becker, M. Oettl, R. Lechner, R. Daniel, J. Finney, and J. C. Smith, *Phys. Rev. Lett.* **93**, 028103 (2004).
- ⁴⁸ H. Tokuhisa, M. Zhao, L. A. Baker, V. T. Phan, D. L. Dermody, M. E. Garcia, R. F. Peez, R. M. Crooks, and T. M. Mayer, *J. Am. Chem. Soc.* **120**, 4492 (1998).
- ⁴⁹ R. E. A. Dillon and D. F. Shriver, *Chem. Mater.* **13**, 1369 (2001).
- ⁵⁰ A. Manna, T. Imae, K. Aoi, M. Okada, and T. Yogo, *Chem. Mater.* **13**, 1674 (2001).
- ⁵¹ A. P. Davis, G. Mab, and H. C. Allen, *Anal. Chim. Acta* **496**, 117 (2003).
- ⁵² G. Lafaye, C. T. Williams, and M. D. Amiridis, *Catal. Lett.* **96**, 43 (2004).
- ⁵³ O. Ozturk, T. J. Black, K. Perrine, K. Pizzolato, C. T. Williams, F. W. Parsons, J. S. Ratliff, J. Gao, C. J. Murphy, H. Xie, H. J. Ploehn, and D. A. Chen, *Langmuir* **21**, 3998 (2005).
- ⁵⁴ M. S. Refat, A. M. El-Didamony, and I. Grabchev, *Spectrochim. Acta, Part A* **67**, 58 (2007).
- ⁵⁵ D. S. Deutsch, A. Siani, P. T. Fanson, H. Hirata, S. Matsumoto, C. T. Williams, and M. D. Amiridis, *J. Phys. Chem. C* **111**, 4246 (2007).
- ⁵⁶ M. L. Moraes, M. S. Baptista, R. Itri, V. Zucolotto, and O. N. Oliveira, Jr., *Mater. Sci. Eng., C* **28**, 467 (2008).
- ⁵⁷ F. Tarazona-Vasquez and P. B. Balbuena, *J. Phys. Chem. B* **108**, 15982 (2004).
- ⁵⁸ D. Xu and K. Schulten, *J. Chem. Phys.* **103**, 3124 (1995).
- ⁵⁹ A. Campa and A. Giansanti, *J. Phys. A* **30**, 1363 (1997).